Please do not adjust margins

ARTICLE

Electronic Supplementary Information (ESI)/ Supplementary Information

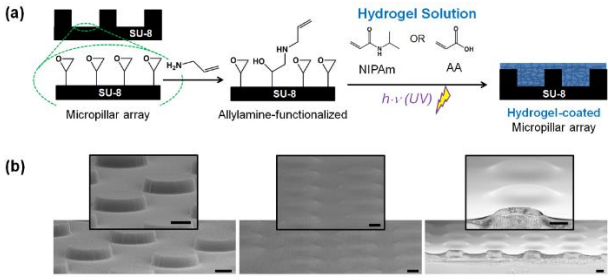

Fig. S1 Sample preparation a) Preparation of Hydrogel Coating on SU-8 photoresist-based micropillar arrays (pillar diameter: 30 μm, centre-to-centre spacing: 60 μm, Pillar height: 10 μm). The hydrogel solution consisting of either N-isopropylamide (NIPAm) or acrylic acid (AA) monomers, initiator, and crosslinker is applied via doctor blading, followed by UV-illumination (Methods). b) SEM images (Methods) of neat unfunctionalized micropillars (left), pillar array coated with hydrogel, dry state (middle), and the cross-section through hydrogel coating (right). All scale bars are 10 μm.

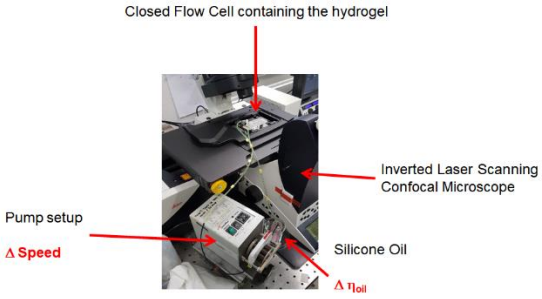

Fig. S2 Experimental setup. The key components are the inverted laser scanning confocal microscope (Leica TCS SP8 SMD), the pump, and the hydrogel coatings in flow cells. The system is not open to the atmosphere. The vials containing the oil and the flow cells are sealed with paraffin tape.

Please do not adjust margins

Please do not adjust margins

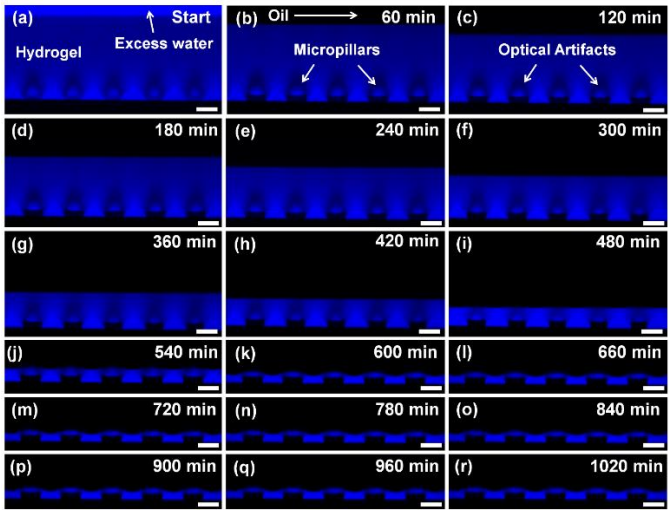

Fig. S3 Linear Shrinkage of PAA-Hydrogels with Oil Flows. Time evolution of side view (*xz*-scan) laser scanning confocal images (40x/1.1 water immersion objective lens) demonstrating progressive dehydration of a hydrogel coating consisting of PAA on a micropillar array (based on SU-8) due to the flow of oil across the coating (flow direction from left to right). The time series consists of images acquired in the fluorescence channel. Only the water (blue) in the hydrogel was dyed using a fluorescent dye (ATTO 488 NHS-Ester, concentration: 1 μg/g). The dye concentration is sufficiently low not to change the interfacial tension. Image acquisition was performed in the middle of the flow channel using a line average of 8 and a scanning frequency of 600 Hz. a) Initially, the hydrogel coating is swollen with fluorescently labelled MilliQ-water and let to equilibrate for 30 min. b-j) Silicone oil (viscosity: 50 cSt, density: 0.96 g/mL) is then continuously circulated over the hydrogel-coated micropillar array at an average flow velocity of 5.3 mm/s. The continuous flow leads to progressive dehydration, *i.e.*, shrinkage, of the hydrogel, evidenced by the decreasing thickness of the fluorescence emission signal detected, representing the thinning of the hydrogel coating. The water leaving the hydrogel coating moves too fast to be monitored. Hence, only the water remaining within the hydrogel contributes to detected fluorescence. k - r) Eventually, the hydrogel reaches a steady-state thickness, which remains unchanged although oil continues to circulate continuously over the hydrogel coating. Pillar dimensions: diameter d = 30 μm, centre-to-centre spacing p = 60 μm, and pillar height h = 10 μm. All scale bars are 30 μm.

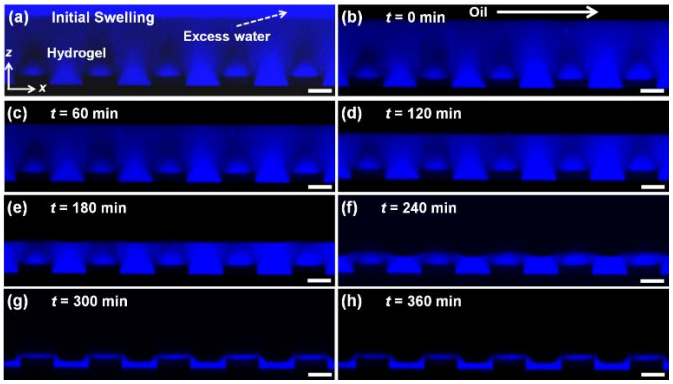

Fig. S4 Linear Shrinkage of PNIPAm-Hydrogels with Oil Flows. Time evolution of side view (xz-scan) laser scanning confocal images (40x/1.1 water immersion objective lens) demonstrating progressive dehydration of a hydrogel coating consisting of PNIPAm with 20% crosslinking density on a micropillar array due to the flow of oil across the coating (flow direction from left to right). The time series consists of images acquired in the fluorescence channel. Only the water (blue) in the hydrogel was dyed using a fluorescent dye (ATTO 488 NHS-Ester, concentration: 1 μg/g). The dye concentration is sufficiently low not to change the interfacial tension. Image acquisition was performed in the middle of the flow channel using a line average of 8 and a scanning frequency of 600 Hz. a) Initially, the hydrogel coating is swollen with fluorescently labelled MilliQ-water and let to equilibrate for 30 min. b-g) Silicone oil (viscosity: 50 cSt, density: 0.96 g/mL) is then continuously circulated over the hydrogel-coated micropillar array at an average flow velocity of 5.3 mm/s. The continuous flow leads to progressive dehydration, *i.e.*, shrinkage, of the hydrogel, evidenced by the decreasing thickness of the fluorescence emission signal detected, representing the thinning of the hydrogel coating. The water leaving the hydrogel coating moves too fast to be monitored. Hence, only the water remaining within the hydrogel contributes to detected fluorescence. g, h) Eventually, the hydrogel reaches a steady-state thickness, which remains unchanged although oil continues to circulate continuously over the hydrogel coating. Pillar dimensions: diameter d = 30 μm, centre-to-centre spacing p = 60 μm, and pillar height h = 10 μm. All scale bars are 20 μm.

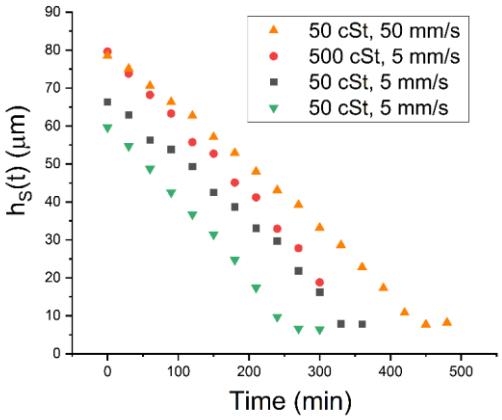

Fig. S5 Representative shrinkage experiments conducted on PNIPAm-based hydrogel coating subjected to a shear flow of silicone oil. Time evolution of the height of the hydrogel coating above the substrate. Summarizing the shrinkage experiments for the PNIPAm-based hydrogel, it appears that neither changing the flow velocity (5 mm/s – 50 mm/s) nor varying the oil viscosity (50 – 500 cSt) strongly affects hydrogel dehydration. Linear shrinkage behavior is evidenced by linear regression. Orange up triangle: R^2 = 0.9972, red solid circle: R^2 = 0.9954, black solid squares: R^2 = 0.9912, green down triangle: R^2 = 0.9972.

This journal is © The Royal Society of Chemistry 20xx

Please do not adjust margins

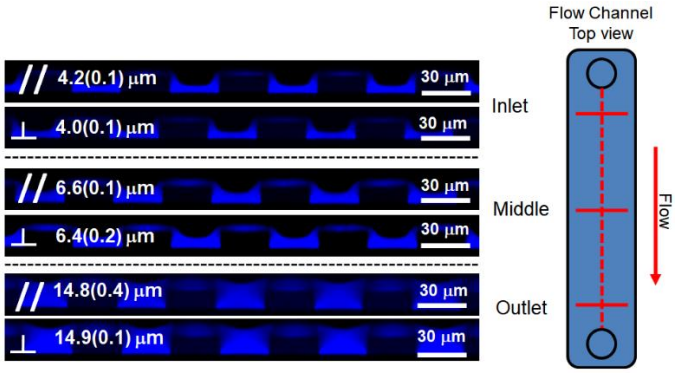

Fig. S6 Progress of shrinkage parallel and perpendicular to the flow direction. Situation of PNIPAm-based hydrogel subjected to a shear flow of 500 cSt silicone oil with an average flow velocity of 10 mm/s after 5 hours. The progress of dehydration close to the inlet is faster than close to the outlet (top view of flow channel on the right). Dehydration slows down in the downstream direction for the same lateral positions (perpendicular to the flow direction).

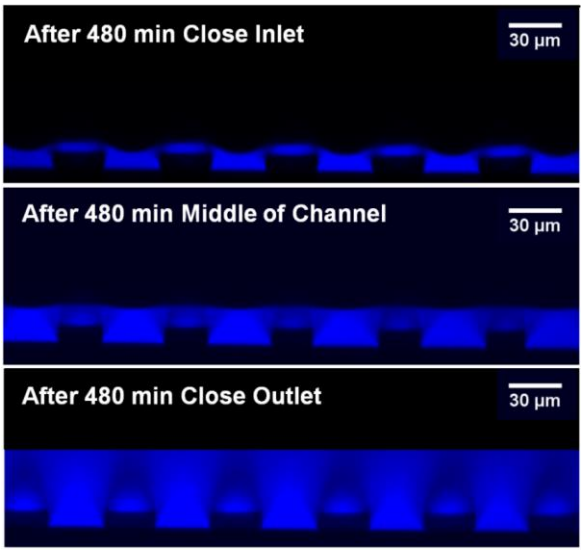

Fig. S7 Progress of shrinkage for PAA-based hydrogels. The progress of dehydration close to the inlet is faster than close to the outlet. After running the shrinkage experiment for 8 hours (480 min, **Figure 2a),** the shrinkage is more advanced close to the inlet than close to the outlet of the flow channel. Close to the inlet, the thickness of the hydrogel coating measured above the substrate amounts to 8.8(0.5) µm. In contrast, in the middle of the flow channel and close to the outlet of the flow channel, the obtained thicknesses of the hydrogel coating amounted to 21(2) µm and 48.4(0.9) µm, respectively.

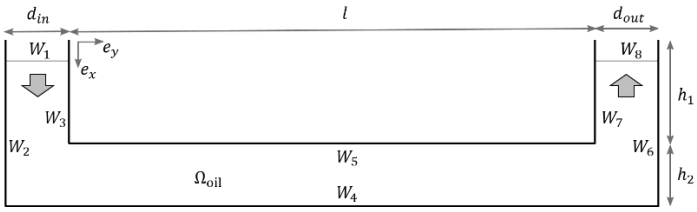

Fig. S8 Computational Domain. The oil is introduced into the domain Ω_{oil} on the left-hand side at W_1 and exits at W_8. e_x and e_y are the unit vectors in x and y direction. The inlet and the outlet have the same width $d_{in} = d_{out} = 3.8\ mm$ and a height of $h_1 = 0.9\ mm$. The flow channel is $l = 53.2\ mm$ long and $h_2 = 0.1\ mm$ high. To close the set of partial differential equations (5) and (9) in the computational domain accurately describing the experimental situation, we define boundary conditions on W_1-W_8 in **Table S1**.

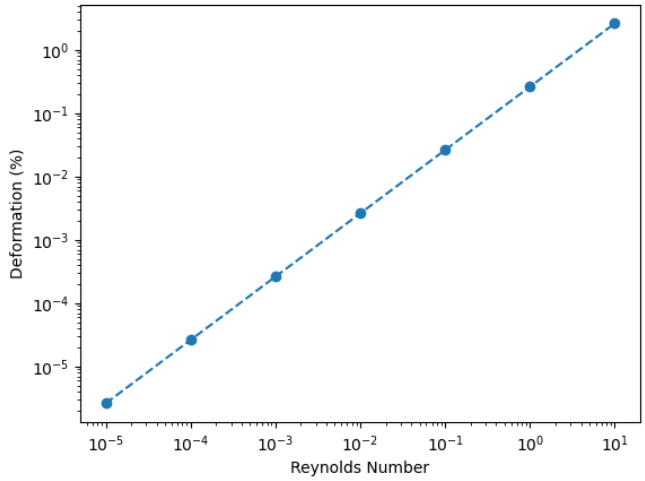

Fig. S9 Hydrogels normal deformation for different Reynolds numbers (*Re*). At experimental flow conditions (*Re* ≈ 10^{-2}) yields a deformation $\epsilon = \tau\ E/2(1+\nu)$ of around 0.02 %. Here, $E \approx 10^6$ Pa and $\nu \approx 0.46$ are the Youngs modulus and the Poisson ratio, respectively.[1, 2]

Table S1. Boundary conditions on Ω_{oil} . Boundaries $W_1 - W_8$ demarcate the computational domain. $\boldsymbol{n}$ and $\boldsymbol{t}$ are the boundaries normal and tangential vectors, respectively. The kinematic flux on W_4 resembles the determined free energy barrier (Eq. 3) and is linearized with respect to c, with $j_0 = 0.1 - 0.16\ mmol/(s\ m^2)$ and $j_1 = 10 - 18\ \mu m/s$. This takes into account that an increased water concentration in the oil gives rise to a reduced thermodynamic driving force, thus reducing the flux.

Boundary	Boundary Type (Momentum)	Boundary Condition	Boundary Type (Mass)	Boundary Condition
W_1	constant inflow	$u_x = 5\ \mathrm{mm/s}$, $u_y = 0$	no normal diffusion	$\nabla \boldsymbol{c} \cdot \boldsymbol{n} = 0$
W_2	no-slip	$u_x = u_y = 0$	no flux	$\boldsymbol{j} = 0$

Please do not adjust margins

W_3	no-slip	$u_x = u_y = 0$	no flux	$\boldsymbol{j} = 0$
W_4	no-slip	$u_x = u_y = 0$	kinematic flux	$\boldsymbol{j} \cdot \boldsymbol{n} = j_0 - j_1 c$
W_5	no-slip	$u_x = u_y = 0$	no flux	$\boldsymbol{j} = 0$
W_6	no-slip	$u_x = u_y = 0$	no flux	$\boldsymbol{j} = 0$
W_7	no-slip	$u_x = u_y = 0$	no flux	$\boldsymbol{j} = 0$
W_8	No normal stress; no lateral flow	$\boldsymbol{n^T} \cdot \boldsymbol{\tau n} = 0,$ $u_y = 0$	no normal diffusion	$\nabla \boldsymbol{c} \cdot \boldsymbol{n} = 0$

S1 Discussion on Free Energy Barrier

We assume that the escape of a water molecule may be viewed as an activated process, for which Kramers' theory can be applied.[3] According to this theory, the escape rate is

$$\tau^{-1} = \frac{\omega_{min}\omega_{max}}{2\pi\zeta}\exp\left(-\frac{\Delta U}{k_B T}\right) = \frac{D\omega_{min}\omega_{max}}{2\pi k_B T}\exp\left(-\frac{\Delta U}{k_B T}\right), \quad (1)$$

where k_B is the Boltzmann constant, T the absolute temperature, ΔU the barrier height, and ω_{min}^2 and ω_{max}^2 are the spring constants describing the harmonic expansion of the barrier potential at the minimum and the maximum, respectively. ζ is the molecule's friction coefficient, which is related to its (tracer) diffusion coefficient D via the Einstein relation $D = k_B T/\zeta$. Furthermore, we assume that for D we can take the tracer diffusion coefficient for water at room temperature, $D \approx 2.3$ nm^2/ns. Furthermore, we assume that the spring constants may be roughly estimated as:

$$\omega_{min}^2 = \omega_{max}^2 = \frac{\Delta U}{\sigma^2}, \quad (2)$$

where σ is the thickness of the oil-water interface, assumed to take the value 1 nm. We thus arrive at

$$\tau^{-1} = \frac{D}{2\pi\sigma^2}\frac{\Delta U}{k_B T}\exp\left(-\frac{\Delta U}{k_B T}\right), \quad (3)$$

From the experimentally measured shrinkage rate and the density of water we may estimate the escape rate as roughly 5 s^{-1}. Inserting numbers, we find

$$\frac{\Delta U}{k_B T}\exp\left(-\frac{\Delta U}{k_B T}\right) = 1.3 \times 10^{-8}, \quad (4)$$

which we may view as a nonlinear equation for $\Delta U/k_B T$. The equation has two solutions, which may be found numerically, and the physically reasonable one is the larger value, $\Delta U/k_B T \approx 21$. In other words, the small shrinkage rate may be explained in terms of a barrier height of order $20\ k_B T$, which we feel is not unreasonable.

Additional References:

1. Y. Jin, T. Yang, S. Ju, H. Zhang, T.-Y. Choi and A. Neogi, *Polymers*, 2020, **12**, 1462.
2. T. Takigawa, T. Yamawaki, K. Takahashi and T. Masuda, *Polym. Gels Netw.*, 1998, **5**, 585-589.
3. H. Risken, in *The Fokker-Planck Equation: Methods of Solution and Applications*, Springer Berlin Heidelberg, Berlin, Heidelberg, 1996, DOI: 10.1007/978-3-642-61544-3_4, pp. 63-95.

This journal is © The Royal Society of Chemistry 20xx

Please do not adjust margins